Carbohydrate Research, 27 (1973) 391–406

THE EFFECTS OF CHANGES IN RING GEOMETRY ON COMPUTER MODELS OF AMYLOSE

ALFRED D FRENCH* AND VINCENT G MURPHY
*Southern Regional Research Laboratory***, *New Orleans, Louisiana 70179 (U S A)*
(Received November 18th, 1972, accepted December 16th, 1972)

ABSTRACT

A review of single-crystal studies shows that α-D-glucopyranose, residues of which constitute the monomeric units of amylose, is flexible within the constraints of the *C1* conformation, and that the internal differences among the rings are most clearly indicated by the variety in ring-torsion angles (or conformation angles) An index of the cumulative effect of changes in these angles is provided by the length of the virtual bond, O-1–O-4, and classification of residue geometries by virtual bond-length permits a systematic selection of suitable residues for the construction of models of amylose By the use of D-glucopyranose residues having different geometries, it is possible to build models of (*a*) V-amylose helices having 6, 7, and 8 residues per turn, (*b*) single and double helical B-amyloses, and (*c*) KBr–amylose, all of which satisfy reasonable stereochemical criteria Because no single residue can satisfactorily model all of the well known polymorphs of amylose, it is suggested that structural determinations that utilize a rigid residue approximation should make use of the full range of known, residue geometries

INTRODUCTION

The importance of residue geometry to polysaccharide modeling has been noted previously[1–4], however, perhaps because no comprehensive exposition of the effects of geometrical variation has hitherto been made, reports on structural determination that either totally neglect or inadequately treat this important variable continue to be published In the present work, therefore, we first correlated virtual bond-length with cumulative changes in residue geometry, and then critically examined the effects of these changes on models of several polymorphs of amylose In this examination, we made use of the criteria of hard-sphere contact of Rees and Skerrett[5] (which are similar to those of Ramachandran *et al* [6]), rather than of potential-energy calculations, because we were primarily interested in determining simply whether a model

*NRC–ARS Post-Doctoral Research Associate
**One of the facilities of the Southern Region, Agriculture Research Service, U S Department of Agriculture

devoid of serious steric strain could be built Such a model would then be a reasonable candidate for further analysis employing X-ray, infrared, or other available data Potential-energy calculations are useful, but, until more-accurate, nonbonded-interaction functions that properly account for intermolecular and hydrogen-bonding effects have been developed, final selection among stereochemically reasonable models should await more conclusive evidence Two recent studies[7,8] offer promise in the direction of the required improvements

SURVEY OF RESIDUE GEOMETRIES

Fig 1 indicates the numbering conventions used herein in discussing the polymorphs of amylose, composed of linear chains of (1*a*→4*e*)-linked α-D-glucopyranose residues Many α-pyranose structures are now available (see Table I) for use in developing models for these polymers, but, in each residue, the positions of the

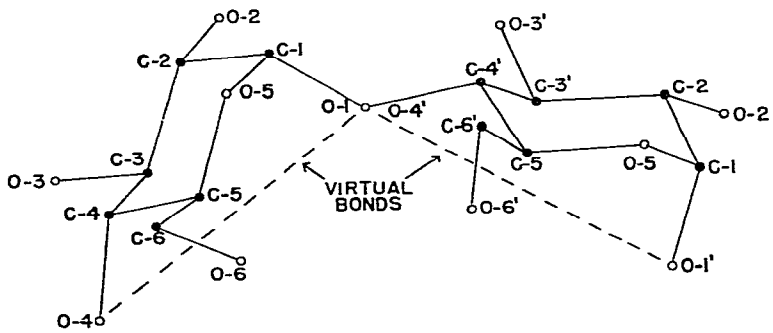

Fig 1 Maltose unit showing the numbering of atoms and the location of the amylose virtual bond (Hydrogen atoms referred to in the text are numbered according to the carbon atom to which they are attached)

terminal oxygen atoms relative both to the center of mass of the ring and to each other are somewhat different As a result, when stereochemically reasonable models for a given polymorph are constructed, the relative orientation of successive residues depends not only upon the repeat distance and number of residues per turn but also upon the choice of residue In order to systematize residue selection, we have found it effective to classify them by the length of the virtual bond, or vector, between O-4 and O-1 (see Fig 1) Table I presents O-4–O-1 distances for α-pyranoses from many sources The range of 10 percent is thought to be reasonably complete, and will be shown to be related to variations in the ring-torsion (conformation) angles

Listed in Table II are pertinent stereochemical data for the α-D-glucose residues in compounds listed in Table I With few exceptions, the conclusions of earlier studies[4,17,30] concerning the constancy of bond lengths and bond angles are confirmed The level of precision in the studies surveyed did vary somewhat, but, despite this variation, the consideration of α-D-glucose rings, only, resulted in torsion-angle

TABLE I

O-4–O-1 VECTOR LENGTHS FOR α-PYRANOSE RESIDUES

Crystal structure	*Code*	*Reference*	*Residue*	*Distance*
Cyclohexaamylose–KOAc	CHA(2)	9	glucose	4 196
α,α-Trehalose dihydrate	—	10	glucose	4 207[a]
Cyclohexaamylose–KOAc	CHA(3)	9	glucose	4 253
Cyclohexaamylose–KOAc	CHA(1)	9	glucose	4 291
α,α-Trehalose dihydrate	—	10	glucose	4 331[a]
Planteose	PLA	11	glucose	4 365
Methyl α-D-glucopyranoside	MeG	12	glucose	4 375
α-L-Sorbose (O-2–O-5)	—	13	sorbose	4 377
Arnott–Scott average residue	ASR	4	glucose	4 400
β-Maltose monohydrate	MAL	14	glucose	4 402
Methyl α-D-mannopyranoside	—	15	mannose	4 405
Raffinose pentahydrate	RAF	16	glucose	4 427
α-Lactose monohydrate	LAC	17	glucose	4 455
α-D-Tagatose (O-2–O-5)	—	18	tagatose	4 455[a]
Dipotassium D-glucosyl phosphate	DGP	19	glucose	4 462
α-D-Xylose	—	20	xylose	4 467
α-D-Glucose–urea	GUR	21	glucose	4 475
α-D-Glucose (neutron diffraction)	ADG	22	glucose	4 485
Methyl α-D-altropyranosice	—	23	altrose	4 502
2-Acetamido-2-deoxy-D-glucose	AGA	24	glucose	4 512
Plant sulfolipid	PSL	25	glucose	4 548
Methyl β-maltoside	MeBM	26	glucose	4 570
1-Kestose	KES	27	glucose	4 575
2-Amino-2-deoxy-D-glucose hydrochloride	GHC	28	glucose	4 583
α-L-Rhamnose monohydrate	—	29	rhamnose	4 587[a]
2-Amino-2-deoxy-D-glucose hydrobromide	GHB	28	glucose	4 607

[a]Value supplied by John Ruble, Department of Crystallography, University of Pittsburgh

ranges of 8–12°, instead of the 16° range cited by Arnott and Scott[4] Some of the older studies yielded values for the O-4–O-1 vector at the extreme ends of the range In the study of 2-amino-2-deoxy-D-glucose hydrobromide[28], for example, the longest O-4–O-1 vector was reported, whereas the pioneering diffractometer study of cyclohexaamylose[9] gave the shortest value in the survey In the latter instance, however, the closed, cyclic structure is thought to strain the residues in just this way[31]

Although there is little, if any, order readily apparent in Table II, a brief study of Dreiding models demonstrated that, as the O-4–O-1 vector lengthens, the torsion angles systematically change More specifically, angles I, II, V, and IV decrease, while III and IV increase (see Table II and Fig 1 for the numbering convention used) It is, of course, possible for angle II, for instance, to increase and the O-4–O-1 vector still to lengthen if other changes more than compensate A simple bookkeeping tool consists in tabulating the quantity $|I|+|II|+|V|+|VI|-|III|-|IV|$, which we call the "torsion-angle index" In Fig 2, the O-4–O-1 distance is plotted against the torsion-angle index for 13 residues That the two variables are related is clearly indicated by the correlation coefficient of the regression line, namely, 0 942 Nitrogen-, phos-

TABLE II

SURVEY OF α-D-GLUCOSE RESIDUES

	Residue Code[a]	CHA2	CHA3	CHA1	PLA	MEG	ASR	MAL	RAF	LAC	DGP	GUR	ADG	AGA	PSL	MEBM	KES	GHC[b]	GHB[b]
Virtual Bond-Lengths	O4-O1	4.196	4.252	4.291	4.365	4.375	4.400	4.402	4.427	4.455	4.462	4.476	4.485	4.512	4.548	4.570	4.575	4.583	4.607
	O3-O1	4.152	4.187	4.171	4.229	4.166	4.232	4.211	4.248	4.263	4.257	4.224	4.280	4.243	4.252	4.218	4.251	4.282	4.232
	O2-O1	2.785	2.795	2.764	2.832	2.809	2.758	2.846	2.780	2.802	2.884	2.796	2.795	2.752	2.743	2.780	2.679	2.733	2.722
Ring Bond-Lengths	C1-C2	1.525	1.505	1.529	1.522	1.526	1.523	1.496	1.513	1.531	1.588	1.517	1.534	1.529	1.514	1.515	1.513	1.543	1.490
	C2-C3	1.500	1.540	1.540	1.511	1.509	1.521	1.545	1.536	1.516	1.546	1.526	1.525	1.536	1.545	1.516	1.520	1.517	1.529
	C3-C4	1.530	1.509	1.524	1.512	1.529	1.523	1.523	1.517	1.533	1.535	1.520	1.518	1.535	1.587	1.529	1.524	1.510	1.521
	C4-C5	1.541	1.546	1.546	1.531	1.525	1.525	1.536	1.516	1.525	1.545	1.524	1.529	1.551	1.518	1.533	1.532	1.541	1.534
	C5-O5	1.451	1.404	1.445	1.430	1.433	1.436	1.467	1.433	1.425	1.480	1.444	1.427	1.460	1.416	1.441	1.441	1.435	1.487
	O5-C1	1.417	1.439	1.425	1.415	1.413	1.414	1.389	1.419	1.443	1.457	1.414	1.425	1.459	1.423	1.408	1.412	1.377	1.404
exo-Ring Bond-Lengths	C1-O1	1.410	1.417	1.400	1.415	1.412	1.415	1.433	1.403	1.387	1.364	1.384	1.389	1.394	1.387	1.415	1.417	1.403	1.425
	C2-O2	1.434	1.412	1.442	1.419	1.421	1.423	1.431	1.424	1.429	1.412	1.423	1.415	1.477	1.369	1.427	1.427	1.509	1.499
	C3-O3	1.427	1.435	1.433	1.436	1.423	1.429	1.436	1.442	1.435	1.422	1.416	1.416	1.451	1.410	1.424	1.429	1.430	1.403
	C4-O4	1.443	1.429	1.409	1.422	1.420	1.426	1.434	1.430	1.436	1.460	1.422	1.425	1.468	1.454	1.435	1.435	1.431	1.456
	C5-C6	1.540	1.533	1.505	1.505	1.507	1.514	1.544	1.519	1.514	1.568	1.504	1.510	1.520	1.513	1.526	1.517	1.527	1.538
Ring Bond-Angles	O5-C1-C2	109.0	109.8	108.1	109.7	110.4	109.2	110.2	109.8	109.7	107.7	110.0	110.1	107.9	112.7	110.9	111.7	109.2	111.2
	C1-C2-C3	109.4	109.2	110.1	109.9	109.8	110.5	109.8	110.9	110.9	105.9	110.9	111.1	110.6	110.1	111.1	111.8	112.5	111.9
	C2-C3-C4	111.1	109.5	109.0	110.0	109.2	110.4	107.0	110.0	110.3	111.2	109.7	109.9	108.6	106.5	106.0	110.4	109.0	108.3
	C3-C4-C5	110.3	110.3	109.8	111.5	110.9	110.2	110.1	110.5	111.1	105.6	109.2	111.2	106.9	110.3	109.2	108.7	106.9	109.5
	C4-C5-O5	108.5	110.3	108.9	110.2	110.2	109.9	107.4	110.9	107.9	110.8	109.8	108.7	105.5	107.8	108.9	107.7	109.0	107.5
	C5-O5-C1	112.0	113.5	115.0	114.5	114.0	113.9	115.6	114.5	114.1	111.3	113.9	113.8	116.6	115.5	114.7	113.1	113.3	111.2
exo-Ring Bond-Angles	O5-C1-O1	111.9	110.9	110.9	109.8	112.7	111.6	108.7	112.7	111.5	116.9	112.0	111.6	108.0	108.6	111.4	112.3	113.5	115.0
	C2-C1-O1	106.7	108.1	106.8	109.9	106.9	108.4	109.3	106.9	108.8	113.1	109.1	109.4	108.3	109.6	107.9	106.3	107.3	108.2
	C1-C2-O2	109.5	110.1	108.7	111.3	111.4	109.3	111.1	111.8	111.1	112.7	111.3	110.9	108.9	111.4	110.2	109.9	109.2	110.3
	C3-C2-O2	112.2	113.2	111.3	109.3	113.2	110.8	110.8	112.2	112.7	110.0	112.4	112.3	108.2	109.4	112.4	111.8	109.4	108.6
	C2-C3-O3	111.3	109.4	110.0	109.6	108.8	109.6	108.3	111.1	107.0	108.9	112.8	108.1	108.1	109.1	110.3	106.7	108.9	109.9
	C4-C3-O3	107.2	108.3	108.5	109.8	110.4	109.7	106.6	107.2	111.6	110.6	112.3	110.6	106.0	109.2	108.7	112.5	111.7	112.5
	C3-C4-O4	106.1	104.8	105.8	110.9	111.6	110.4	110.9	111.9	110.5	103.3	111.8	108.3	107.8	108.5	111.1	110.4	109.8	111.7
	C5-C4-O4	107.9	108.1	108.3	108.2	106.4	108.6	105.6	106.7	107.2	103.3	106.2	110.9	106.0	110.7	109.4	110.9	110.7	109.0
	C4-C5-C6	108.4	110.7	111.3	109.8	112.0	112.7	111.5	113.8	113.7	106.6	114.5	111.6	113.8	111.7	111.8	114.5	111.5	113.1
	O5-C5-C6	104.5	106.5	107.1	108.0	107.8	106.9	105.8	107.4	107.2	114.1	108.2	108.1	105.0	110.5	106.4	107.5	105.2	106.4
Ring[c] Torsion-Angles	O5-C1-C2-C3 (I)	59.9	58.5	58.4	58.2	58.2	56.9	58.6	55.6	53.9	61.2	55.4	54.1	53.3	53.7	56.3	50.6	53.0	56.6
	C1-C2-C3-C4 (II)	-53.9	-55.9	-57.2	-55.1	-55.6	-53.5	-58.6	-53.6	-51.2	-62.1	-54.5	-51.2	-59.0	-53.7	-58.5	-49.8	-53.3	-53.6
	C2-C3-C4-C5 (III)	52.1	53.6	55.5	52.5	54.2	52.5	58.9	52.5	53.5	60.5	55.2	53.3	63.4	58.6	60.5	55.4	56.7	56.2
	C3-C4-C5-O5 (IV)	-54.5	-55.1	-55.7	-52.3	-54.1	-54.8	-57.3	-54.3	-57.5	-59.1	-57.4	-57.5	-62.9	-60.3	-60.0	-61.4	-62.4	-60.7
	C4-C5-O5-C1 (V)	63.1	59.7	60.8	57.5	58.0	61.4	58.8	59.0	62.9	64.0	61.1	62.2	63.8	60.1	58.2	64.5	66.2	63.4
	C5-O5-C1-C2 (VI)	-66.0	-62.5	-61.9	-60.8	-60.1	-62.0	-60.2	-59.4	-61.6	-63.6	-59.5	-61.0	-58.7	-57.9	-56.2	-59.2	-59.4	-61.5

[a] See Table I for explanation of residue codes [b] Oxygen-2 is replaced by a nitrogen atom in these structures [c] Torsion angle A-B-C-D is defined as the clockwise angle from bond A-B to bond C-D when the 4 atoms are projected onto a plane perpendicular to bond B-C and atom A is closest to viewer.

phorus-, and sulfur-substituted rings were not included in this analysis, primarily because their structures have not as yet been so accurately determined That torsion angles cannot vary independently of bond lengths and bond angles is recognized, but torsion angles appear to be the most sensitive indicators of the ring distortion accompanying a change in virtual bond-length, and the torsion-angle index offers a means of gauging the degree of this distortion

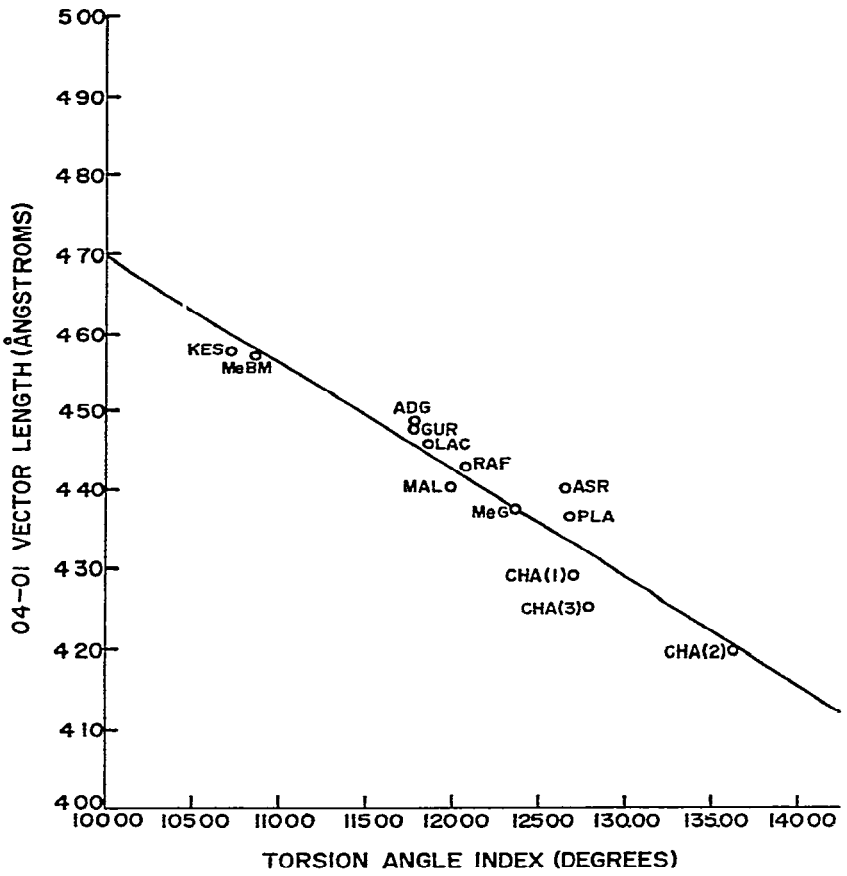

Fig 2 Plot of virtual bond-length *versus* torsion-angle index for α-D-glucopyranose residues (containing only carbon, hydrogen, and oxygen) (The regression line has a slope of 75° per Å, and a correlation coefficient of 0 942)

It must be concluded that there is a considerable degree of geometrical freedom within the constraints of the *C1* conformation Therefore, as emphasized by Arnott and Scott[4], in performing potential-energy or diffraction-intensity calculations, there is no justification for allowing a large variation in the glycosidic angle while maintaining a rigid residue The residue geometry, itself, is a more logical variable It would, of course, be of interest to know the causes of deformation of the ring geometry. Two

of the structures surveyed, GUR and ADG (see Table I for residue coding), contain an unsubstituted α-D-glucopyranose molecule, but, in GUR, a strong hydrogen-bonding agent, urea, is present Despite the different hydrogen-bonding and packing schemes, the molecular geometries are quite similar A third crystal-structure containing unsubstituted D-glucopyranose (the monohydrate) has been reported in preliminary form[32], and it is characterized by an O-4–O-1 distance of 4 49 Å, this value is very similar to those for GUR (4 475 Å) and ADG (4 485 Å) Substitution patterns do, however, appear to influence residue geometry, as may be seen by comparing MeG with ADG, and MeBM with MAL (in Table II) It is also likely that the presence of ions has some effect, because the three identically substituted CHA residues differ slightly As accurate crystal structures of saccharides become more plentiful, rules governing residue deformation will, presumably, be deduced For the present, however, we surmise that the presence of such complexing agents as methyl sulfoxide or potassium bromide need not cause changes in molecular parameters outside the range currently observed

CONSTRUCTION OF MODELS

The computer model-building program evolved from one written by Jackobs[33] In this program, the residue is considered to be a rigid body attached to a virtual bond, or vector, extending from O-4 to O-1, and use is made of the monomer-equivalence postulate[34] According to the latter, once an initial residue is properly located relative to a fiber axis, a simple screw operator is all that is required to generate the rest of the chain Thus, if $\tilde{X}_i$ is the position vector for an atom in the ith residue, then

$$\tilde{X}_{i+1} = R\tilde{X}_i + L, \tag{1}$$

where R and L respectively define a rotation about, and a translation parallel to, the fiber axis For a chain having n residues and p turns per repeat distance f, the angle θ through which a residue must be rotated to generate the next unit is

$$\theta = \frac{2\pi p}{n}, \tag{2}$$

and the translation h is

$$h = |f/n| \tag{3}$$

By convention, in a right-handed, coordinate system, n is positive or negative depending on whether the chain is right- or left-handed If a Cartesian-coordinate system is specified in which the z axis serves as the fiber axis, then

$$R = \begin{bmatrix} \cos\theta & -\sin\theta & 0 \\ \sin\theta & \cos\theta & 0 \\ 0 & 0 & 1 \end{bmatrix} \quad \text{and} \quad L = \begin{bmatrix} 0 \\ 0 \\ h \end{bmatrix} \tag{4}$$

When the chain is generated in this way, and the O-4–O-1 vectors from the residues of a single repeat are projected onto the x–y plane, an equilateral figure (*e g* , a regular hexagon in the instance of a 6-residue, single-turn helix) is formed in which the distance d from the origin to the midpoint of each side can be shown to be

$$d = |\sqrt{(b^2 - h^2)}/2 \tan(\theta/2)|, \tag{5}$$

where b is the length of the virtual bond It is clear, then, that the length of the virtual bond and the helical parameters n, p, and f completely determine the locations of all O-4–O-1 vectors in the model To locate the associated atoms, there need only be specified the rotational positions of the residues about these vectors and the locations of any side groups (*e g* , the primary alcohol grouping attached to C-5) that have rotational freedom Because only polymers that are thought to form regular helices are here under consideration, all residues in a given model are rotated equally about their respective O-4–O-1 vectors In principle, this still permits the residue to assume an infinite number of positions, however, as will be seen later, the direct relationship between rotational position and the steric criteria severely limits the range of possibilities

In our work, the following computational procedure was found convenient After reading-in n, p, f, and a set of atomic coordinates derived from an appropriate, single-crystal study, the initial residue was first placed so that its O-4–O-1 vector was bisected by the origin Rotational operators were then used to bring the x–y projection of O-1 onto the y-axis and to elevate the residue such that

$$Z_{O-1} - Z_{O-4} = h \tag{6}$$

At that point, the desired rotation of the residue about the O-4–O-1 vector was effected, the reference position being the one in which the O-1–O-4–C-6 plane coincided with the y–z plane, a positive rotation being clockwise when viewed from O-4 to O-1 Having thus properly oriented the initial residue, it only remained to translate it a distance $\pm d$ along the x axis and to generate the rest of the chain *via* the operation described in equation (1) The translation was positive for a right-handed model and negative for a left-handed one

Once the full model had been constructed, it was examined for stereochemical feasibility (here, "feasible" implies reasonableness of glycosidic angle and absence of severe, short contacts between nonbonded atoms) For the most part, the latter are possible only between atoms on contiguous residues, but, in the case of compact structures, such as the V-amyloses, the primary alcohol group can also interact with residues distant by about one turn of the helix The construction of our program was such that both the rotation of the residue about the virtual bond and the position of the primary alcohol group could readily be varied in attempts to derive a stereochemically sound model Generally speaking, in any such model-building study, the most confidence is usually placed in the value of the crystallographic repeat-distance obtained from fiber-diffraction photographs Decreasing confidence is held in the helical parameters n and p and in such residue parameters as side-group position,

rotation about a virtual bond, and specific residue-geometry A comprehensive study must allow reasonable variations in all of these parameters

MODELS OF V-AMYLOSE

An informative means of illustrating the effects of various residue-geometries on computer models is to plot the glycosidic angle against the amount of residue rotation about the virtual bond Fig 3 is such a graph for left-handed, six-residue V-amylose, a polymorph having six residues repeating in 7.95 Å Four different

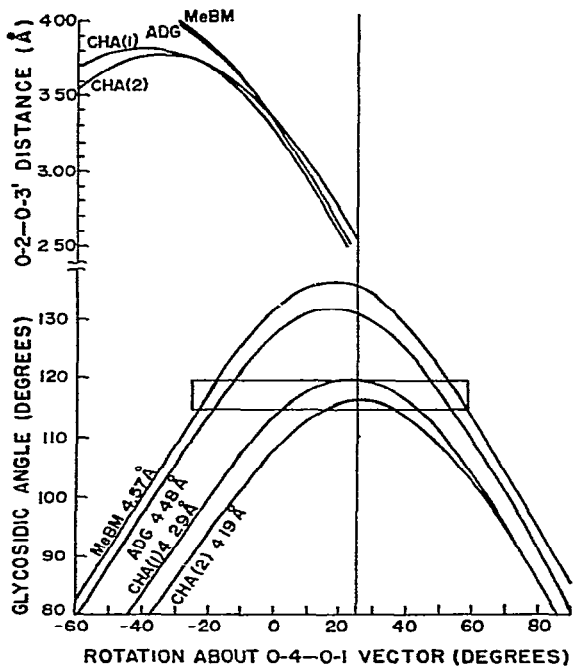

Fig 3 Values of glycosidic angle and O-2–O-3 distance for left-handed, six-residue-per-turn V-amylose models [Four different residues are included that encompass the observed range of O-4–O-1 vector lengths CHA(3) residue helices, having 4 25-Å virtual bonds, yield a curve intermediate to the CHA(2) (4 19 Å) and CHA(1) (4 29 Å) residue models The CHA(3) curve intersects the zone of reasonable glycosidic angle at a residue rotation that suggests a strong hydrogen-bond between O-2 and O-3′, and that also agrees with X-ray results[35 36] The vertical line at about 20° of residue rotation on this and following Figures indicates the maximum allowed residue rotation due to the O-2–O-3′ contact]

residues having O-4–O-1 distances of 4 19, 4 29, 4 48, and 4 57 Å are included, thereby covering the full range of virtual bond-lengths observed At a given value of residue rotation, it is apparent that the glycosidic angle increases when the O-4–O-1 distance increases Deviations of the family of curves from a completely parallel set are caused by differences in ring geometry other than those which affect only virtual bond-length

Reasonable models for amylose are expected[4] to have a glycosidic angle lying between 115 and 120°, the range bounded by the rectangles in the Figures For V-amylose, the full extent of residue rotations that produce reasonable glycosidic angles is indicated by the intersections of the curve for the longest vector residue with the zone of reasonable glycosidic angle To determine whether or not the entirety of the resultant 80° residue-rotation range is stereochemically viable, a contact analysis is performed. For the V polymorphs, the O-2–O-3′ distance is quite dependent on residue geometry However, as indicated on a separate scale in Fig 3, differences are quite small in the important range of strong hydrogen-bonding If a minimum, hydrogen-bounded contact of 2 5 Å is accepted, then the realistic residue rotations must be limited to those less than 25° Below −10° of residue rotation, however, C-5–C-6′ and other short contacts are present, leaving only the range from −10 to +25° with the desired combination of reasonable glycosidic angle and no short contacts

A recent X-ray study[35 36] indicated that a residue rotation of 15° gives the best agreement between observed and calculated diffraction-intensities At this value, models made with the CHA(3) residue (4 25 Å virtual bond) have a glycosidic angle of 118°, and a distance of 2 85 Å between O-2 and O-3′ that is indicative of a hydrogen bond In the absence of diffraction information, however, it would be inappropriate to limit consideration to models that feature this hydrogen bond The lack of such an intra-chain, hydrogen bond could conceivably be offset by inter-helical bonding in the solid state or by solvation in solution

SEVEN- AND EIGHT-RESIDUE V-AMYLOSES

When precipitated from solution with molecules bulkier than those of butyl alcohol, amylose forms crystalline complexes that have been deduced to have the amylose component arranged as a helix repeating in 8 Å with seven or eight residues per turn[37–42] Sundararajan *et al*[43] suggested that it is necessary to utilize a glycosidic angle of 110° to construct a compact, seven-residue helix using averaged CHA residues, whereas Goebel *et al*[1] reported that a seven-residue helix is energetically and geometrically feasible if the MeBM residue is used Fig 4 shows that both are correct, and also suggests that neither of the structures proposed is optimal from the standpoint of the completely isolated helix With the short-vector, CHA(2)-residue models, no glycosidic angle greater than 108° is obtained, regardless of contact criteria The use of the long vector (4 57 Å), MeBM residue yields models having glycosidic angles of up to 128°, but, at the value of residue rotation where the glycosidic angle is 117°, the O-2–O-3′ distance is 3 5 Å At the residue-rotation value of 15°, where the O-2–O-3′ bond would be strongest, model helices constructed from the ASR averaged residue have a glycosidic angle of 118° Because optically active structures containing seven residues per repeat must lack crystallographic symmetry, it is anticipated that there would be geometrical differences among the residues, and the structure of ASR residues already described would only be the most reasonable

starting-point in a structural analysis In this regard, it is interesting that, on the basis of unit-cell dimensions, Simpson *et al* [40] proposed an elliptical shape for the seven-residue helices

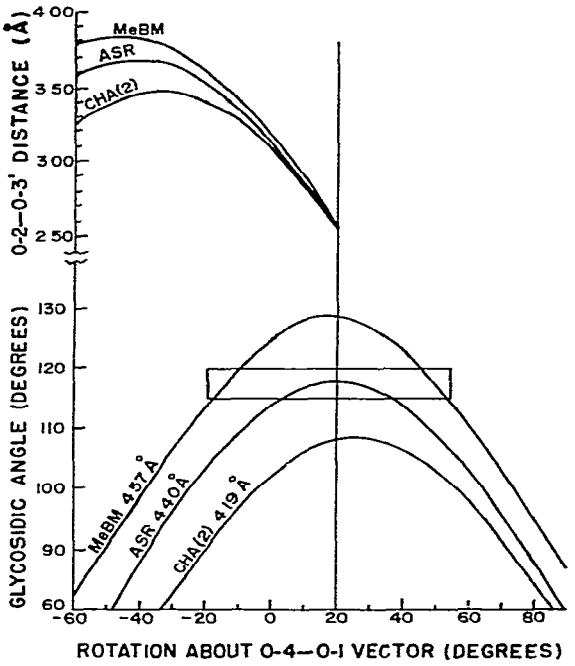

Fig 4 Graph of glycosidic angle and O-2–O-3′ distance for left-handed, seven-residue V-amylose models using three different residue geometries [CHA(2) residues are geometrically incapable of forming seven-residue V-helices having a glycosidic angle large enough to be considered reasonable, and the MeBM-residue, model helices have glycosidic angles that are too large at values of residue rotation where an O-2–O-3′ hydrogen-bond would have significant strength The selectively averaged ASR residue meets the conditions of reasonable glycosidic angle with an O-2–O-3 distance indicative of a hydrogen bond, but it should be noted that no evidence has been presented for this hydrogen bond in the seven-residue structure]

Fig 5 indicates similar relationships for models of eight-residue, compact helices Models constructed with the short vector (4 19 Å), CHA(2) residue have unreasonably small glycosidic angles and, in addition, suffer from a very short H-1–H-4′ contact On the other hand, models based on the longer vector (4 485 Å), ADG residue have satisfactory glycosidic angles, no short contacts, and an O-2–O-3′ distance representative of a strong hydrogen-bond As only the longer vector residues can lead to models having reasonable glycosidic angles, the allowed range of residue rotation is small compared to those for the six- and seven-residue, compact helices Yamashita and Monobe[42] determined that the eight-residue, V helix has tetragonal symmetry, so no more than two different residues can be involved Coupled with the observation of very limited range of residue-rotation, this type of symmetry suggests the formation of at least a weak O-2–O-3′ hydrogen bond

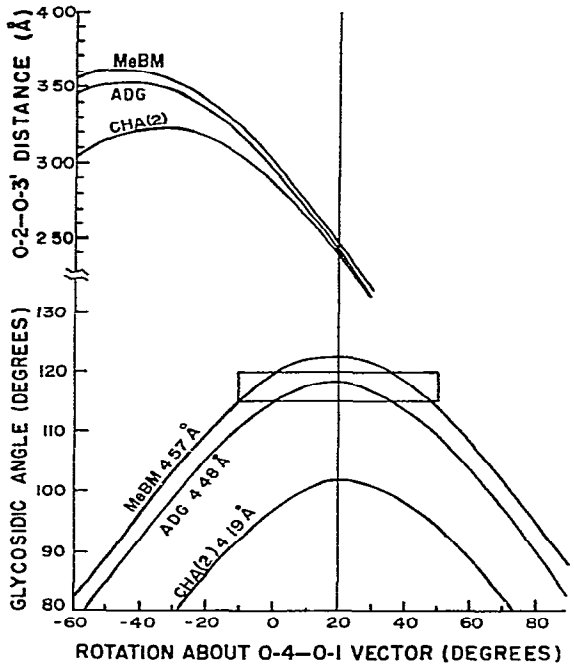

Fig 5 Graph for left-handed, eight-residue, V-amylose models, using three different residue geometries [Only the longer vector residues have geometries suitable for construction of these models, leaving only a narrow range of allowed-residue rotation Within this range, all O-2–O-3′ distances are less than 3 2 Å, suggesting that at least a weak hydrogen-bond is formed ADG residues (4 48 Å) form the most satisfactory eight-residue helices, whereas the MeBM residues would be more suited to the formation of the (unreported) nine-residue structures]

B-AMYLOSE

Proposals for the structure of B-amylose, the native polymorph of some starches, include two-[44], three-[45], four-[46], and six[47]- residue, single helices, all repeating in 10 5 Å, and a double helix composed of two six-residue strands[48] Each strand of the double-helical model proposed repeats in 21 0 Å, but is related to the other strand by a two-fold rotation-axis giving a crystallographic repeat of 10 5 Å From the maximum length of the ring vector, it is obvious that more than two residues are needed in order to satisfy the 10 5 Å repeat. The latest crystallographic evidence favors helices in which the number of residues per turn is evenly divisible by three, owing to the established presence of a sixth-order, meridional reflection[47] and the possible presence of a very weak, third-order reflection[49]. These data notwithstanding, the four-residue model was examined (in addition to the others) in order that no reasonable proposal should be overlooked

Despite the use of a wide range of residue geometries, however, we found that no three- or four-residue model could be constructed without steric strain Three-

residue models suffer from numerous, over-short contacts, including H-5–H-4′ or H-1–O-3′ for left-handed chains, and H-1–C-6′ or H-3–H-4′ for right-handed chains Indeed, only by increasing the bridge angle to 135° can models having three residues per 10 5 Å be made to be free from interference Four-residue, B-amylose models are somewhat less crowded than the three-residue variety, especially when one of the shorter ring-vector residues is the basis of construction, but, even then, they are still unacceptable according to the criteria of Rees and Skerrett[5] Very short H-5–C-6′ or O-2–O-3′ distances eliminate the left-handed models, and C-1–C-6′ or H-3–O-3′ contacts show the right-handed models to be unlikely Here again, though, the use of a glycosidic angle of 135° would permit the construction of otherwise unstrained models

Six-residue models fare considerably better For the single-helix case, short-vector residues permit construction of stereochemically feasible, right-handed models, and either long or short vector residues may be used to build reasonable, left-handed models In the latter, however, only the shorter residues lead to an O-2–O-3′ distance that could be construed as a hydrogen bond Both right- and left-handed, double-helix models are also stereochemically feasible, they require long vector residues, such as ADG, to attain reasonable glycosidic angles For example, with the CHA(3) residue (4 25 Å virtual bond), the largest angle attainable is about 106° The best double-helical models of both chiralities have no contacts in the disallowed region, and few or none in the marginally allowed, moreover, in neither case is there any problem due to interference between the two strands of the structure

KBr—AMYLOSE

The polysaccharide chains of the KBr–amylose complex contain four residues in 16 1 Å Jackobs *et al* [33] reported structure-factor calculations for this polymorph by using a model constructed from ADG residues having a bridge angle of 108° As they obtained a fairly high value for the reliability index, and as stereochemical criteria not then available place 108° outside the acceptable range, it was of interest to examine four-fold helices composed of other residues Table III presents the more interesting parameters of some left-handed models. At −70° of residue rotation, where the 108° angle occurs for the ADG model, longer vector residues lead to only slightly different values for the glycosidic angle, moreover, no available residue, regardless of geometry, can produce a model that does not exhibit steric strain to a certain degree Rotation of the residue by ~20° in the positive direction relieves the cramping (see Table III) in models based on the longer vector residues, and, in these cases, also yields a glycosidic angle in the acceptable range Short vector residues produce C-1–C-3′ and H-1–C-3′ contacts throughout the range of good glycosidic angle, and this is no doubt responsible for the high potential-energy reported for models using CHA geometry[1] Like Jackobs *et al* [33], we could not construct a right-handed model containing four residues in 16 1 Å that did not involve serious crowding of the primary alcohol group

TABLE III

CHARACTERISTICS OF LEFT-HANDED MODELS OF KBr–AMYLOSE

Residue	*Rotation of residue (degrees)*	*Glycosidic angle (degrees)*	*C-1–C-3′ 3 0[a] (Å)*	*C-1–O-3′ 2 7[a] (Å)*	*H-1–O-3′ 2 2[a] (Å)*
ADG, 4 48 Å	−70	108 4	2 85	2 58	1 87
	−60	112 9	2 95	2 72	2 01
	−50	117 5	3 04	>2 80	2 14
	−40	122 0	3 11	>2 80	2 24
MeBM, 4 57 Å	−70	107 8	3 01	2 71	1 89
	−60	112 9	3 12	>2 80	2 05
	−50	118 2	>3 20	>2 80	2 21
	−40	123 3	>3 20	>2 80	2 35
KES, 4 57 Å	−70	110 6	3 02	>2 80	2 07
	−60	115 7	3 13	>2 80	2 23
	−50	120 9	>3 20	>2 80	2 37
	−40	125 9	>3 20	>2 80	>2 40
CHA(3), 4 25 Å	−30	113 1	2 83	2 55	1 76
	−10	117 0	2 87	2 61	1 78
	10	118 3	2 84	2 58	1 70
	30	116 2	2 73	2 48	1 53
ASR, 4 40 Å	−50	111 8	2 97	2 73	1 96
	−40	115 7	3 04	>2 80	2 05
	−30	119 3	3 09	>2 80	2 11
	−20	122 3	3 12	>2 80	2 14

[a]Minimum, "marginally allowed", contact distance[5]

Models of extended conformations, such as the KBr polymorph, appear to be especially sensitive to variations in residue geometry The models using CHA(3) residues show a satisfactory glycosidic angle over a sixty-degree range of residue rotation, and the ADG and MeBM residue models exhibit satisfactory angles in a narrow range of angles, similar to each other but quite removed from the range for the CHA(3) models In addition, despite the fact that the KES and MeBM residues have almost identical O-4–O-1 distances, models based on the former are considerably less crowded, as is indicated by a difference of 0 2 Å for the H-1–O-3′ distance at comparable residue rotations

DISCUSSION

Classification of α-D-glucopyranose residues on the basis of O-4–O-1 vector lengths appears to be a very useful, if not rigorous, device for introducing residue geometry as a variable in the structural analysis of poly(1*a*→4*e*)saccharides Indeed, it would seem useful to have comparable indices available for other types of linkages and for other sugars that afford polysaccharides. For ready reference, virtual bond-lengths for other glycosidic linkages have also been included in Table II With the exception of the selectively averaged ASR moiety, all of the residues that we have

considered correspond to actual conformations observed for smaller molecules; therefore, a polymer model constructed from any one of these must be considered reasonable if it meets the steric and crystallographic requirements Furthermore, it is probable that the range of variation in residue geometry considered is adequate to define models as either feasible or not, especially if some small tolerances are allowed in the hard-sphere restrictions As it has been shown that geometrically different residues are needed for the construction of satisfactory models for the various polymorphs of amylose, no single kind of residue can be regarded as being "typical" of amylose

The chief advantage of the virtual-bond, helix-construction method is that, when the fiber-repeat distance is known, only structures that meet that requirement receive consideration Methods that use rotation about the glycosidic linkages afford a single map that contains all possible combinations of repeat distance and number of residues per repeat For any given combination, however, each representation of this type provides only four (or fewer) possible models For example, were the map based on MeBM geometry and a glycosidic angle of 117°, two of the possible models for an eight-residue helix repeating in 8 Å would correspond to the intersections of the MeBM curve (in Fig 5) with a horizontal line through 117°, and the other two would correspond to the intersections on the analogous drawing for right-handed structures Separate maps are needed for each residue considered and for each value of the glycosidic angle Even assuming invariant residue-geometry, Figs 3 and 4 and Table III indicate that, in some cases, variation of the glycosidic angle within the allowed range produces a substantial range of residue rotations In such instances, in order to obtain meaningful results by use of methods that involve rotation about the glycosidic bonds, it would be necessary to examine maps made at many small increments of glycosidic angle Therefore, the virtual-bond method can require much less computation and can facilitate comparisons between alternative geometries

Under favorable circumstances, the type of study reported here may be useful in predicting the most satisfactory residue for modeling a given structure For example, diffraction-intensity calculations were initially made for V-amylose by using a model composed of ADG residues[35 36] Error functions showed the residue rotation to be ~15°, which can be seen (in Fig 3) to correspond to a glycosidic angle of 132° As this value is considerably outside the accepted range, some doubt was cast upon the validity of the structural determination Subsequent calculations revealed, however, that the intensity-error function was fairly insensitive to the residue geometry and that, in the favored rotation range of 10–20°, models composed of CHA residues had quite reasonable glycosidic angles (again, see Fig 3) On stereochemical grounds, it would therefore appear that the true structure of the monomeric units of six-residue V-amylose is more closely approximated by the shorter vector residues

Another area in which the present results are of utility is in discussing the reported conversion of the seven-residue V-amylose into the six-residue structure Previous workers[43] have suggested that conversion is accomplished by a small

change in the dihedral angles about the glycosidic linkage, accompanied by an increase in the angle itself from 110° to 119° A comparison of the models deemed most likely, from our work, for the six-, seven-, and eight-residue V-amyloses indicated that, during conversion, the glycosidic angle, residue rotation, and O-2–O-3′ distance can retain optimal values if the residue is permitted some geometrical flexibility, as this reasoning is more compatible with the evidence available for small molecules, it is believed to be the more likely explanation

Both the six-residue, single- and double-helical models for B-amylose remain undiscredited by these modeling computations However, until more evidence than that from single-geometry, potential-energy computations is presented, acceptance of either model as factual is attended by considerable uncertainty

REFERENCES

1 C V Goebel, W L Dimpfl, and D A Brant, *Macromolecules*, 3 (1970) 644
2 D A Brant and W L Dimpfl, *Macromolecules*, 3 (1970) 655
3 D A Rees, *Biochem J*, 125 (1971) 86P
4 S Arnott and W E Scott, *J Chem Soc, Perkin Trans, II*, (1972) 324
5 D A Rees and R J Skerrett, *Carbohyd Res*, 7 (1968) 334
6 G N Ramachandran, C Ramakrishnan, and V Sasisekharan, in G N Ramachandran (Ed), *Aspects of Protein Structure*, Academic Press, London, 1963, p 121
7 P Zugenmaier and A Sarko, *Kolloid Z Z Polym*, 250 (1972) 434
8 R L McCullough and P H Lindenmeyer, *Kolloid Z Z Polym*, 250 (1972) 440
9 A Hybl, R E Rundle, and D E Williams, *J Amer Chem Soc*, 87 (1965) 2779
10 G M Brown, D C Rohrer, B Berking, C A Beevers, R O Gould and R Simpson, *Acta Crystallogr, Sect B*, 28 (1972) 3145
11 D C Rohrer, *Acta Crystallogr, Sect B*, 28 (1972) 425
12 H M Berman and S H Kim, *Acta Crystallogr, Sect B*, 24 (1968) 897
13 S H Kim and R D Rosenstein, *Acta Crystallogr*, 22 (1967) 648
14 G J Quigley, A Sarko, and R H Marchessault, *J Amer Chem Soc*, 92 (1970) 5834
15 B M Gatehouse and B J Poppleton, *Acta Crystallogr, Sect B*, 26 (1970) 1761
16 H M Berman, *Acta Crystallogr, Sect B*, 26 (1970) 290
17 D C Fries S T Rao, and M Sundaralingam, *Acta Crystallogr, Sect B*, 27 (1971) 994
18 S Takagi, Ph D Thesis, University of Pittsburgh (1971)
19 C A Beevers and G H Maconochie, *Acta Crystallogr*, 18 (1965) 232
20 A Hordvik, *Acta Chem Scand*, 25 (1971) 2175
21 R L Snyder and R D Rosenstein, *Acta Crystallogr, Sect B*, 27 (1971) 1969
22 G M Brown and H A Levy, *Science*, 147 (1965) 1038
23 B M Gatehouse and B J Poppleton *Acta Crystallogr, Sect B*, 27 (1971) 871.
24 L N Johnson, *Acta Crystallogr*, 21 (1966) 885
25 Y Okaya, *Acta Crystallogr*, 17 (1964) 1276
26 S C Chu and G A Jeffrey, *Acta Crystallogr*, 23 (1967) 1038
27 G A Jeffrey and Y J Park, *Acta Crystallogr, Sect B*, 28 (1972) 257
28 S C Chu and G A Jeffrey, *Proc Roy Soc, Ser A*, 285 (1965) 470
29 R C G Killean, J L Lawrence, and V C Sharma, *Acta Crystallogr, Sect B*, 27 (1971) 1707
30 H M Berman, S C Chu, and G A Jeffrey, *Science*, 157 (1967) 1576
31 D French, *Advan Carbohyd Chem*, 12 (1957) 253
32 R C G Killean, W G Ferrier, and D W Young, *Acta Crystallogr*, 15 (1962) 911
33 J J Jackobs, R R Bumb, and B Zaslow, *Biopolymers*, 6 (1968) 1659
34 G Natta and P Corradini, *Nuovo Cimento, Suppl*, 15 (1960) 9
35 A D French and B Zaslow, *Chem Commun*, (1972) 41
36 A D French, V G Murphy, and B Zaslow, manuscript in preparation
37 R S Bear, *J Amer Chem Soc*, 66 (1944) 2122

38 B ZASLOW, *Biopolymers*, 1 (1963) 165.
39 Y YAMASHITA AND N NIRAI, *J Polym Sci, Part A-2*, 4 (1966) 161
40 T D SIMPSON, F R DINTZIS, AND N. W TAYLOR, *Biopolymers*, 11 (1972) 2591
41 F. R SENTI AND S R ERLANDER, in L MANDELCORN (Ed), *Non-Stoichiometric Compounds*, Academic Press, New York, 1964, p 567
42 Y YAMASHITA AND K MONOBE, *J Polym Sci, Part A-2*, 9 (1971) 1471
43 P R SUNDARARAJAN AND V. S R RAO, *Biopolymers*, 8 (1969) 313
44 R E RUNDLE, L DAASCH, AND D FRENCH, *J Amer Chem Soc*, 66 (1944) 130
45 D R KREGER, *Biochim Biophys Acta*, 6 (1951) 406
46 L C SPARK, *Biochim Biophys Acta*, 8 (1952) 101
47 J. BLACKWELL, A SARKO, AND R. H MARCHESSAULT, *J Mol Biol*, 42 (1969) 379
48 K KAINUMA AND D FRENCH, *Biopolymers*, 11 (1972) 2241
49 A D FRENCH, unpublished results